Design and Optimization of 3D Compact Stripline and Microstrip Bluetooth/WLAN Balun Architectures Using the Design of Experiments Technique

Daniela Staiculescu[1], *Member, IEEE,* Nathan Bushyager[1], *Student Member, IEEE,* Ade Obatoyinbo[2], *Member, IEEE,* Lara J. Martin[3], *Member, IEEE* and Manos M. Tentzeris[1], *Senior Member, IEEE*

***Abstract*— In this paper, various architectures of 3D compact microwave balanced to unbalanced (balun) transformers for Bluetooth/WiFi antenna applications are successfully designed and optimized using the Design of Experiments (DOE) approach. Two different multilayer topologies, one microstrip and one stripline, are investigated on Low Temperature Co-fired Ceramic (LTCC) substrate. The design goals for both baluns are perfectly balanced outputs from 2 to 3 GHz and a resonant frequency of exactly 2.4 GHz. It is demonstrated, using only eight simulations, that perfectly balanced outputs are not possible under the given conditions in the case of the microstrip balun. Nevertheless, the stripline balun can be optimized due to its almost symmetrical structure, and both simulations and measurement results verify the conclusions. The DOE method is very simple to implement and gives a clear understanding of the system behavior at the beginning of the design process, reducing the amount of work required for achieving the design goals by orders of magnitude compared to the widely used trial-and-error approach. The matching and unique measurement issues regarding the calibration, placement of probes and the de-embedding of the microstrip to coplanar waveguide (CPW) transitions are discussed in detail for the optimized stripline balun. This technique can be easily applied to the fast and efficient optimization of complicated radiation structures, such as reconfigurable or multilayer mutliband antenna arrays.**

***Index Terms*—3D Balun, CPW Lines, Design of Experiments (DOE), LTCC, Microstrip Lines, Multilayer Modules, Optimization Algorithms, WiFi/Bluetooth Antennas.**

I. Introduction

The objective of this paper is to explore the design, optimization and implementation of 3D multilayer baluns for antenna applications as a benchmark for the efficiency of this approach. Two 2.4 GHz multilayer baluns in microstrip and stripline technologies are optimized using DOE and the prototypes are built and tested in a 20 layer LTCC process.

In recent years it has become increasingly important to find ways to move certain components off-chip, with the drive towards System On Package (SOP) solutions that have demonstrated tremendous potential in developing compact RF modules [1], [2]. In these geometries, a significant portion of the passive elements are located not on-chip (where possible), but rather on-package thereby saving chip real estate, improving performance, and reducing cost since the package is inevitably cheaper than the corresponding semiconductor material. The demands for compactness and functionality, as well as the close proximity of these passives to the antenna [3], especially for 802.11x/Bluetooth compact modules, make the design and optimization processes of such systems more and more challenging.

II. DOE Background

Existing optimization packages included in commercial electromagnetic simulators, often do not take into account the specific effect of each of the factors involved in the design process and the degree of interaction between them, thus leading to time-consuming "trial-and-error" approaches. For the complicated 3D architectures of RF/microwave multilayer modules, such as reconfigurable antenna arrays or mutiband 3D implemented planar radiating topologies, a comprehensive and sophisticated tool is necessary to account for complex phenomena such as coupling and fringing effects. Alternative optimization methods suited to this kind of complexity are Neural Networks [4] and Genetic Algorithms [5]. These are very precise methods which unfortunately require a hefty amount of prior knowledge and are computationally complex and time consuming. Design of Experiments (DOE) [6], [7] overcomes these disadvantages. It provides a thorough understanding of all of the factors involved in the design process, and identifies which are more significant, which are not significant at all, how they interact with each other, and if the goals are achievable in the given conditions. Most importantly, the method is very easy to implement with negligible computational overhead. This method is suited as a first approach to understand the behavior of a system, to decide whether an optimization is possible under certain conditions and filter out all the insignificant factors from the

Manuscript received June 17th, 2004. This work was supported in part by NSF CAREER ECS-9984761, the NSF ECS-0313951 under Grant BS123456, the Georgia Electronic Design Center (GEDC) and the NSF-GT Packaging Research Center (PRC)

[1]Daniela Staiculescu, Nathan Bushyager and Manos M. Tentzeris are with the Georgia Electronic Design Center, School of ECE, Georgia Institute of Technology, Atlanta, GA, 30332, U.S.A. (email: daniela@ece.gatech.edu)

[2]Ade Obatoyinbo is with HRL Laboratories LLC, Malibu, CA, 90265, U.S.A.

[3]Lara Martin is with Motorola, 8000 Sunrise Boulevard, Plantation, FL, 33322, U.S.A.

beginning of the process [8]. Also, in combination with Response Surface Modeling (RSM), DOE is a successful optimization technique [9]. If very accurate models and very precise optimization are required, more sophisticated methods like Neural Networks and Genetic Algorithms come into play.

A design of experiments (DOE) is a series of tests in which a set of input variables or factors is purposely changed so that the experimenter can observe and identify the reasons for changes in the output response. Previous work has demonstrated the advantages of the use of design of experiments in the modeling and optimization of RF/microwave circuits [10]. A very important result of a DOE analysis of a system is the explicit effect of each of the factors involved in the design process, as well as all the interactions between them.

The most popular designs for achieving this goal are the factorial experiments, which involve several factors and whose goal is the study of the joint effects of the factors on a response. Prior knowledge of the analyzed system and of the fabrication process is required for choosing the factors and their studied ranges. The 2^k factorial design is the simplest one, with *k* factors at *2* levels each. The two levels of each of the *k* variables, "-" and "+", represent the lower and the upper limits of the interval in which the variable is analyzed and they are determined by the variations/tolerances of the fabrication process, as well as by the space and material limitations of the multilayer module. The 2^k factorial designs are useful in the preliminary analysis of the system, when there are many factors that might affect the system. They provide the smallest number of runs for studying *k* factors and are widely used in factor screening experiments [6].

This paper shows the first use of the DOE in a feasibility study of the optimization of a circuit. In other words, for the two balun topologies presented in the previous section, it will be demonstrated that, under the given design conditions, the microstrip balun cannot completely satisfy the balance design requirements for any frequency between 2-3 GHz that is different than the design frequency within the specified degree of tolerance. This is a very important "a-priori" conclusion, in any case a designer tries to achieve the unachievable. When confronted with such challenges, the designers often spend a lot of time trying to get results rather than just do a systematic factor screening at the beginning of the design process.

The DOE approach steps are as follows: first, electromagnetic analysis of the system helps identify the important factors to be considered. Then these factors are included in a factorial experiment and the outputs are obtained and recorded using a full-wave time-domain simulator. The preliminary DOE analysis gives a general understanding of how factors affect performance and how they interact with each other, and quantifies the significance of all the factors, to be able to eliminate from the analysis the ones that are not significant and keep only the most significant ones when the design resources are limited. Explicit statistical models are developed for each of the outputs as a function of the inputs, the optimization constraints are afterwards applied to these models and the values of the input variables that best satisfy all of them are calculated.

III. BALUN BACKGROUND

Baluns - from BALanced to UNbalanced transformer - are required in a wide variety of microwave components, such as balanced mixers, push-pull amplifiers, multipliers, phase shifters and antennas [11] [12], [13], [14],. A balun basically transforms a single-ended network to a differential one or vice-versa. Baluns have been actively studied since the work done in the area by Marchand [15]. Active baluns have been reported [16] but are plagued by the problem of high DC power consumption, noise figure and limited power handling capability. MMIC baluns of different forms have also been reported in the literature but implementing relatively sizeable structures on chip rather than on package (where possible) increases the cost of the final product substantially. Lumped element implementation of MMIC baluns (on chip) [17] have likewise been studied but suffer from the same problems as any of the on chip baluns reported – lumped or distributed.

Other methods that have been examined for baluns are suspended substrate techniques, [18] which were impossible to fabricate in monolithic form, and other topologies [19], that required inhomogeneous dielectric layers and thus could only be implemented in non-standard processes.

3D approaches have the advantage of saving substrate space by using the third dimension. SOP multilayer implementations [2] have demonstrated very good performance with a higher level of integration on multilayer substrates such as LTCC.

In order to save space on the substrate, one alternative is to implement the lines as spirals. This way, the size of the overall structure is reduced. The disadvantage of such structures is the unwanted couplings between the spiral turns. In this case, the parasitic capacitance resulting from the spiral turn coupling compensates for part of the quarter or half wavelength long straight lines. Therefore, further size reduction is achieved with the spiral implementation.

Apart from the use of spiral lines for space reduction, baluns can also be implemented using different technologies. This work specifically focuses on microstrip and stripline balun development using a 20-layer LTCC substrate with the following characteristics: $\varepsilon_r = 7.8$, $\tan\delta = 0.005$, layer thickness = 3.7 mil.

Fig. 1 presents the exploded view of the stripline balun. Layers 0 and 4 represent the ground planes of the structure. The half wavelength open line is on layer 2. A small portion of this line is placed on layer 3 to avoid overlapping traces and to take advantage of the multilayer configuration for overall size reduction. One of the quarter wavelength coupling sections is on layer 1 and the other on layer 3. Each of these lines is shorted to the ground planes (through vias) above and below it respectively. The top ground plane is patterned in order to allow for signal lines from each of the input and output ports (on the buried layers) to be connected to the top of the structure through vias for probing by a coplanar probe. Vias (not shown in figure) are used to connect the top ground plane to the bottom, to keep both ground planes (upper and lower) at the same potential.

A similar balun was designed in microstrip topology as shown in Fig. 2. In this configuration, the ground plane is

buried in layer 3 (since there is no top ground plane). The half wavelength section (open line) is now located on the top layer (layer 0) as well as the co-planar waveguide probe pads, which allow for probing with co-planar probes at each of the ports. The remaining section of the spiral open line is now on layer 2 and is connected as before through vias. Layer 1 contains both coupled quarter wavelength sections whose outputs are connected to layer 0 and are terminated on the ground plane on layer 3 (through vias).

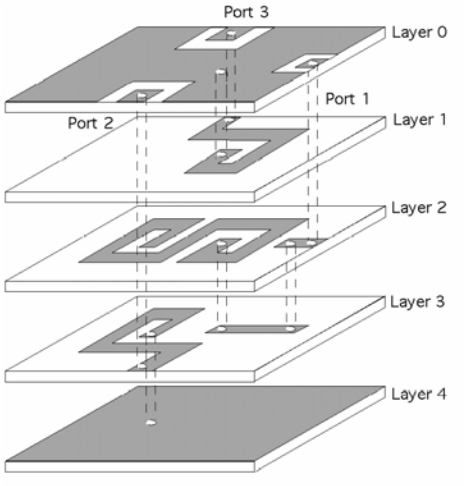

Fig. 1. Stripline implementation of spiral balun.

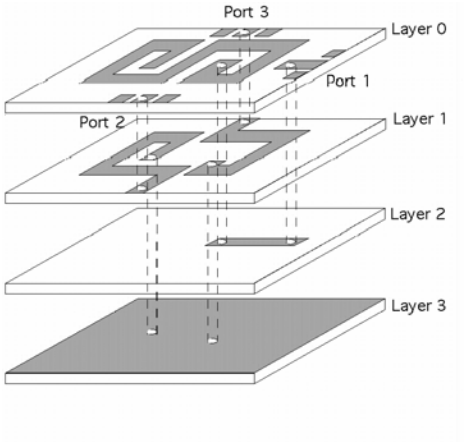

Fig. 2. Microstrip implementation of spiral balun.

The layout of these structures is quite challenging since the close proximity of the turns introduces parasitics and sometimes destroys the symmetry of the topology. Conventional optimization approaches would require the variation of a large number of geometrical parameters and a very large number of simulations. In this paper, the Design of Experiments (DOE) technique was applied in the beginning of the design process for a thorough understanding on how various design parameters can be modified to achieve optimal performance. The design goals were a resonant frequency of 2.4 GHz, as well as excellent amplitude balance (better than ± 0.5 dB) and a consistent phase imbalance (better than ± 5 deg) at the output from 2-3 GHz. It was expected that the optimization of the stripline topology would be easier due to its symmetry. Also, since the outputs are located on different layers, good isolation characteristics between ports 2 and 3 are expected. However, with the microstrip topology, the structure is not symmetric and the port 3 line is slightly shortened compared to the port 2 line. This is due to the fact that the via that connects the portion of the open line on layer 2 to the rest of the line on layer 0 restricts the length of the port 3 line, as it can be seen in Fig. 2.

IV. Microstrip Balun Optimization

The first case to be considered was the microstrip topology, which is of great interest due to its wide use in RF and microwave circuits. The preliminary simulations of the structure in Fig. 2 showed poor amplitude balance between ports 2 and 3, as shown in Fig. 3. detailed look at the field distribution shows that there is a lot of coupling at the center of the structure. This is due to the fact that the central part of the open line on Layer 0 does not couple with the short lines on Layer 1 (see Fig. 2) and causes parasitic coupling with the neighboring lines on the open spiral line. Also, strong coupling is present between the corners of the spiral open on Layer 0 and the two lines connecting the shorts to the ports 2 and 3 on Layer 1. All of these coupling effects are illustrated in Fig. 4 on a top view of the structure.

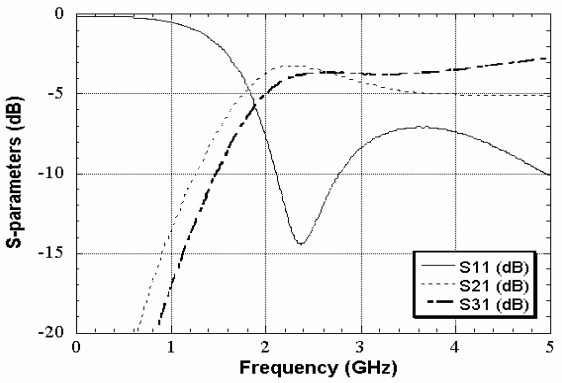

Fig. 3. S-parameters of initial microstrip balun.

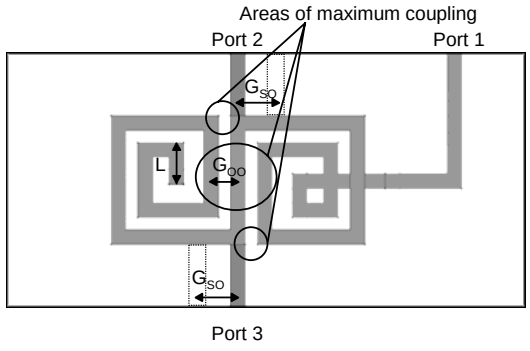

Fig. 4. Top view emphasizing the coupling effects of microstrip balun and the factorial experiment variables.

Therefore, two factors were initially identified for the experiment: G_{oo}, or the open-to-open gap, and G_{so}, or the distance the output lines for ports 2 and 3 are moved from the initial position for coupling reduction, as shown in Fig. 4. A third factor L, representing the length by which the lines are shrunk at one end, was added to the experiment for compensating the imbalance between S_{21} and S_{31}. More preliminary simulations showed that other possible factors, like the number of turns and the distance between turns do not change the results significantly. So a full factorial experiment with three factors consisting of $2^3 = 8$ treatment combinations was run. The two levels chosen for each input variable were controlled by the fabrication process and are presented in Table I.

TABLE I.
VARIABLES FOR THE 2^3 EXPERIMENT

Variable	L (mil)	G_{so} (mil)	G_{oo} (mil)
"-" level	0	0	6
"+" level	30	13	19

The output variables chosen were Δ_{2GHz} and Δ_{3GHz}, which are the differences between S_{21} and S_{31} at 2GHz and 3GHz respectively, as well as the resonant frequency f_{res}. The phase imbalance is not recorded at the two frequencies since the variation in the band is not monotonic and the results at the edges of the bandwidth are not relevant. Instead, the worst value of the phase imbalance in the frequency band, P_w, is recorded. The optimization goal was: $\Delta_{2GHz} = 0$; $\Delta_{3GHz} = 0$; $P_w = 0$; $f_{res} = 2.4$ GHz.

The eight simulations were run in the MicroStripes TLM-based Modeler and the results are presented in Table II.

TABLE II.
2^3 EXPERIMENT

Run	L	G_{so}	G_{oo}	f_{res} (GHz)	Δ_{2GHz} (dB)	Δ_{3GHz} (dB)	P_w (deg)
1	-	-	-	2.37	1.4	0.7	16
2	+	-	-	2.42	1.1	0.8	21
3	-	+	-	2.37	1.2	0.5	12.5
4	+	+	-	2.42	0.9	0.9	18
5	-	-	+	2.29	1.6	0.6	17
6	+	-	+	2.40	1.0	0.9	23
7	-	+	+	2.30	0.9	0.7	14
8	+	+	+	2.41	0.8	0.9	18

The Analysis of Variance (ANOVA) statistical analysis [6] was performed using JMP statistical software [20]. ANOVA reveals the statistical significance of all the input variables and of their interactions and generates regression models of the outputs as a function of the inputs. In this case:

$$\Delta_{2GHz} = 1.125 - 0.1625\left(\frac{L-15}{15}\right) - 0.1625\left(\frac{G_{so}-6.5}{6.5}\right) \quad (1)$$

$$\Delta_{3GHz} = 0.75 + 0.125\left(\frac{L-15}{15}\right) \quad (2)$$

$$P_W = 17.4375 + 2.5625\left(\frac{L-15}{15}\right) - 1.8125\left(\frac{G_{so}-6.5}{6.5}\right) \quad (3)$$

The statistical analysis of the model shows which parameters are significant for each of the three figures of merit and the ones that are not significant are eliminated from further analysis. The first order prediction models presented in equations (1) - (3) were validated for model assumptions of normality and equal variance of the residuals [6].

These models can be used to predict the performance of the system for a specific configuration, or to optimize the balun performance with respect to either figure of merit or combinations of the three. The initial goal of this optimization was to have $\Delta_{2GHz} = 0$ and $\Delta_{3GHz} = 0$ simultaneously. Since L was a significant factor for all three prediction models, G_{so} was fixed at the most convenient levels for achieving the optimal performance (13 mil), and the two derived values needed for L to satisfy both $\Delta_{2GHz} = 0$ and $\Delta_{3GHz} = 0$ were $L_{2GHz} = 104$ mils and $L_{3GHz} = -75$ mils. These two conditions could not be satisfied at the same time, and this rendered the optimization of the microstrip balun impossible under the described ideal conditions. The two transmission coefficients for ports 2 and 3 could not satisfy the balance requirements in the studied bandwidth (2 - 3 GHz) because the two lines had to be shrunk and elongated at the same time. On the other side, the optimized solution for more relaxed specifications, such as Δ_{2GHz} and Δ_{3GHz} <0.5 dB or <1dB could be easily identified and are given in Table III without the need for additional simulations.

TABLE III.
VARIABLE VALUES TO SATISFY MORE RELAXED OPTIMIZATION SPECIFICATIONS.

Specification	0.5 dB	1 dB
L_{2GHz}	57.7	11.5
L_{3GHz}	-15	45

The data in Table III shows that the length required to satisfy the 2GHz condition is decreasing and the one required to satisfy the 3GHz condition is increasing for more relaxed specifications. The $L_{2GHz} = L_{3GHz}$ is calculated from the regression models to be satisfied for a 0.84 dB amplitude imbalance condition. So this particular structure has been optimized as follows: if an amplitude imbalance up to 0.84 dB can be tolerated within the minimum and maximum frequencies, the following are the optimized values for the three variables: $G_{oo} = 6$ mil, $G_{so} = 13$ mil and $L = 26$ mil. The phase imbalance for these factor values, calculated using equation (3), is found to be 17.5 degrees, again not in the widely accepted range of ± 5 deg. L has a relatively larger influence on the phase performance compared to G_{so} and has to be minimized for optimal phase imbalance. According to equation (3), optimal phase is achieved for $L = -76$ mil, so L has to be decreased to decrease the phase imbalance. Run number 4 of Table II does not ensure optimal phase performance; rather run number 3, with the same values for G_{so} and G_{oo} but minimum L, is the optimal for phase performance, presenting a maximum phase imbalance of 12.5 degrees at 2.4 GHz, while maintaining the amplitude imbalance below 1.2dB. One would have to pick the optimal values for the three optimization parameters depending on the

design requirements and specifications (higher significance of amplitude or phase balance).

Last but not least, a successful weighted optimization for the microstrip balun was performed for the three figures of merit presented in equations (1) – (3), plus the resonant frequency f_{res} with an optimization goal of 2.4 GHz. First, a statistical model was developed for the resonant frequency. The analysis revealed that all three main effects were statistically significant as well as the two-factor interactions $L \cdot G_{oo}$ and $G_{so} \cdot G_{oo}$. The first order model developed based on the data presented in Table II is:

$$f_{res} = 2.3725 + 0.04\left(\frac{L-15}{15}\right) + 0.0025\left(\frac{G_{so}-6.5}{6.5}\right) - 0.0225\left(\frac{G_{oo}-12.5}{6.5}\right) + 0.015\left(\frac{L-15}{15}\right)\left(\frac{G_{oo}-12.5}{6.5}\right) + 0.0025\left(\frac{G_{so}-6.5}{6.5}\right)\left(\frac{G_{oo}-12.5}{6.5}\right) \quad (4)$$

and was validated for model assumptions of normality and equal variance of the residuals. The optimization tool used is based on the maximum desirability method pioneered by Derringer and Suich [21] and included all four variables in the prediction models (1) – (4). For this particular optimization, the importance was weighted as follows: resonant frequency and the phase imbalance, which showed high values in the previous analysis, were weighted with a factor of importance of 5, and the two amplitude imbalances with a factor of importance of 1. This is an abitrary choice and can be changed according to specific design needs. The optimized values of the four figures of merit, as well as the values of the three factors, are presented in Table IV.

TABLE IV.
OPTIMIZATION RESULTS

Δ_{2GHz} (dB)	Δ_{3GHz} (dB)	P_w (deg)	f_{res} (GHz)	L (mil)	G_{oo} (mil)	G_{so} (mil)
0.95	0.75	15.6	2.395	15	6	13

Fig. 5 shows the intersection of the surfaces represent the possible values of L, G_{oo} and G_{so} that satisfy the optimization conditions.

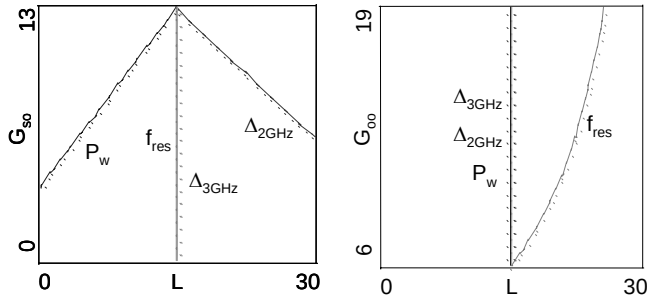

Fig. 5. The intersection of the surfaces that represent the possible values of L, G_{oo} and G_{so} that satisfy the optimization conditions.

Obviously, a trial-and-error approach where the designer changes the factors in a random manner could not have given the same insight after only eight simulations. Genetic algorithms often require hundreds of simulations for optimization, while the trial-and-error approach can not give an understanding of the system after a very large number of simulations, especially when interactions are involved.

V. STRIPLINE BALUN OPTIMIZATION

In the stripline case, the optimization included only two factors of the three illustrated in

Fig. 4: G_{oo}, or the open-to-open gap, and G_{so}, or the distance the output lines for ports 2 and 3 are moved from the initial position for coupling reduction, since there was no need to compensate for any asymmetry in the geometry. A simple 2^2 experiment was run for the same values of the two variables as the ones shown in Table I. The results of the experiment are presented in Table V. It can be seen that there is very small variation with these factors for the stripline configuration. The structure is symmetric and there are not too many unwanted couplings that affect the performance. The simulation results of the initial design, with the two output lines for the balanced ports not staggered (G_{so} = 0), and the distance from the center line to the first spiral turn equal to 6 mils (G_{oo} = 6), are shown in Fig. 6.

The balun was fabricated and the de-embedded measurements demonstrated very good agreement with the simulations for both the amplitude and phase imbalance, as shown in Fig. 7 and Fig. 8. The amplitude imbalance is less than 0.5 dB and the phase balance better than 5 degrees in the frequency range of interest, so this stripline balun corresponds to the design requirements mentioned earlier.

TABLE V.
2^2 EXPERIMENT

Run	G_{so}	G_{oo}	f_{res} (GHz)	Δ_{2GHz} (dB)	Δ_{3GHz} (dB)	$P_{2.4GHz}$ (deg)
1	-	-	2.42	0.05	0.15	0
2	-	+	2.42	0.2	0	1.2
3	+	-	2.35	0	0.1	0
4	+	+	2.42	0.18	0.13	2.2

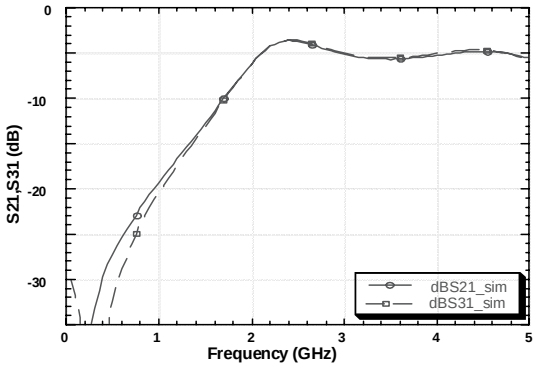

Fig. 6. Simulation results for S21 and S31 of the stripline balun.

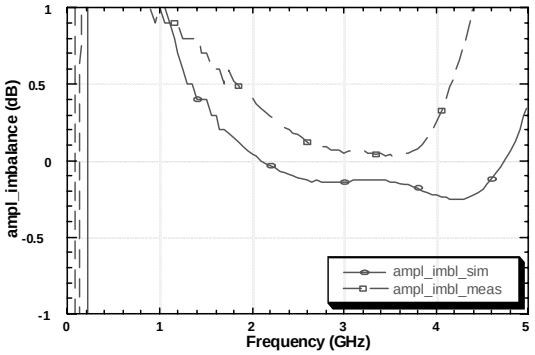

Fig. 7 Amplitude imbalance measurement vs. simulation for the stripline balun.

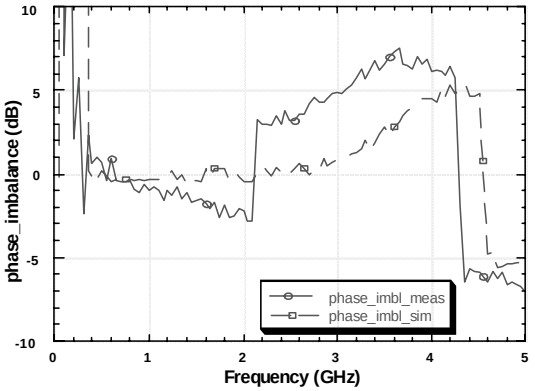

Fig. 8 Phase imbalance measurement vs. simulation for the stripline balun.

VI. Balun De-Embedding and Matching

The structures presented in the preceding section were all simulated using EM software without considering the transitions from the edge of the structure – usually in a buried layer - to the top (layer 0) where they are probed. In most modules, the edge of the geometry is connected to the top layer (for probing with a co-planar probe) through a via and some length of transmission line. Therefore, de-embedding structures have to be designed and fabricated in order to have an accurate experimental characterization.

Fig. 9 shows one de-embedding structure for the signal line located on layer 3.

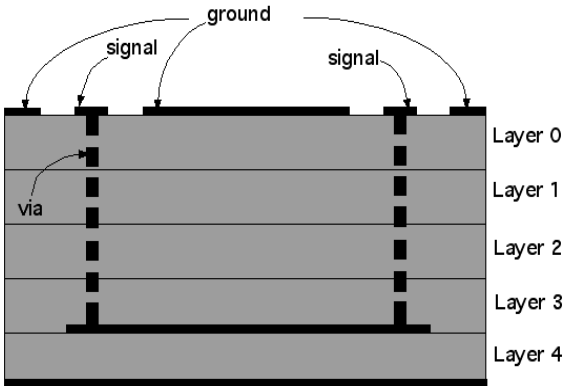

Fig. 9. De-embedding structure for signal line on layer 3.

First, the de-embedding structure is measured and its S-parameters recorded. These S-parameters are used to model the structure as a symmetric 2-port device in Advanced Design System (ADS) [12]. Then the balun itself (which contains the transition intrinsically) is measured. Finally, the symmetric device is split into two and cascaded in ADS on each side of the measured balun S-parameter block. All are simulated using the de-embedding function of ADS, and then the de-embedded balun S-parameters are obtained.

The deembedding structures were characterized and modeled using various components including simple inductors resistors and capacitors as well as ADS models of microstrip and stripline transmission lines.

A simple equivalent-circuit model of the deembedding structure used for the stripline balun is shown in Fig. 10.

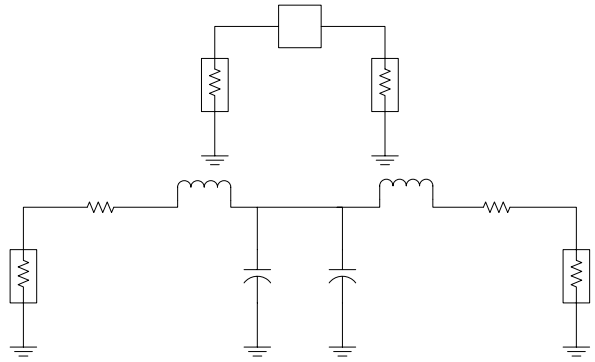

Fig. 10. Circuit model for the deembedding structure.

Another important issue in the optimization of 3D baluns is the matching. A balun is basically a power divider that performs the additional function of phase inversion at one of its output ports. Another way of looking at it is that it provides a constant 180^{O} phase difference between the output ports. From the theory of power dividers and three-port networks, it is clear that it is impossible to construct a three-port network that is matched at all ports, lossless, and reciprocal [22]. Since all passive networks are reciprocal (including the baluns under discussion) and can for the most part be treated for ease of analysis as lossless networks, it is therefore clear that the baluns in this study cannot be matched at all ports.

In fact since one of the design criteria used for the balun was matching at the input port, and since the output ports are designed for equal power split, one can expect a desired output of –3dB. Of course this would be the ideal case, where all losses were ignored. In reality, the data shows outputs on the order of –3.5dB to –3.8dB, which corresponds to a worst case loss of 0.8dB.

The ideal return loss for each of the output ports is –6dB [23]. The impedance at port 1 is 50Ω, while the impedance at each one of the two balanced ports each is 100Ω. Thus, each of the output ports sees 50Ω (input) in parallel with 100Ω (the other output port), leading to a 33.33Ω equivalent impedance. The return loss is defined as:

$$\Gamma = \frac{Z_L - Z_c}{Z_L + Z_c} = \frac{100 - 33.3}{100 + 33.3} = 0.5 = -6dB$$

The actual measured value of the return loss is –5.7dB at each of the output ports. The output port mismatch can be solved by adding a resistive network between the output ports [23].

VII. Conclusion

The Design of Experiments approach has been combined with full wave EM simulations first for studying the feasibility of the optimization of two multilayer baluns and then for optimizing the feasible one for WiFi/Bluetooth frequency ranges. Two spiral baluns have been designed in microstrip and stripline topologies. For the microstrip topology, it was found that it was not possible to obtain satisfactory amplitude and phase balances for the entire frequency band, but the resonant frequency can be optimized if no tough requirements are imposed on the imbalances. For the stripline topology, optimization was achieved and test structures were fabricated to validate the simulations. It has to be noted that in both cases the amount of required simulations was a very small fraction (more than an order of magnitude) with respect to any other optimization approaches.

By extending the Design of Experiment (DOE) approach to the system-level modeling and optimization of complex topologies, such as 3D multilayer modules or packaging-adaptive antenna arrays, at the beginning of the design process, the designer can save a lot of time, shorten the design cycle of added functions and achieve the design goals in a simple and elegant manner, while incorporating variations of the fabrication/material processes and eliminating "trial-and-error" deficiencies.

Acknowledgement

The authors wish to acknowledge the support of the NSF CAREER ECS-9984761, the NSF ECS-0313951, the Georgia Electronic Design Center (GEDC) and the NSF-GT Packaging Research Center (PRC).

References

[1] J. Laskar, A. Sutono, C.-H. Lee, M. Davis, M. Maeng, N. Lal, K. Lim, S. Pinel; M. Tentzeris, A. Obatoyinbo, "Development of integrated 3D radio front-end system-on-package (SOP)" – *2003 GaAs IC Symp. Dig.*, pp. 215 -218, Oct. 2001.

[2] C.-H. Lee, A. Sutono, S. Han, K. Lim, S. Pinel, E.M. Tentzeris, J. Laskar: "A compact LTCC-based Ku-band transmitter module"**,** *IEEE Trans. Components, Packaging & Manufacturing Technology* , vol. 25, pp. 374 – 384, Aug. 2002.

[3] R.R.Tummala, V. Sundaram, F. Liu, G. White, S. Hattacharya, R.M. Pulugurtha, M. Swaminathan, S. Dalmia, J. Laskar, N.M. Jokerst, Y.-C. Sang: "High density packaging in 2010 and beyond", *Proc. of the Symp. on Electronic Materials and Packaging*, pp. 30 -36, Dec. 2002.

[4] R. Hecht-Nielsen: "Neurocomputing", New York, Addison-Wesley, 1990.

[5] N. Chaiyaratana, A.M.S. Zalzala: "Recent developments in evolutionary and genetic algorithms: theory and applications", *Second International Conference On Genetic Algorithms In Engineering Systems, Innovations And Applications*, pp. 270 -277, Sept. 1997.

[6] D.C. Montgomery, *Design and Analysis of Experiments*, New York: J. Wiley & Sons, 1997.

[7] D.S. Boning, P.K. Mozumder: "DOE/Opt: a system for design of experiments, response surface modeling, and optimization using process and device simulation"**,** *IEEE Trans. Semiconductor Manufacturing*, pp. 233–244, May 1994.

[8] N. Bushyager, D. Staiculescu, A. Obatoyinbo, L. Martin, M. M. Tentzeris, "Optimization of 3D Multilayer RF Components Using the Design of Experiments (DOE) Technique", *2004 IEEE MTT-S Int. Microwave Symp. Dig.*, pp. 1859-1862, June 2004.

[9] N. Bushyager, D. Staiculescu, L. Martin, N. Vasiloglou, M.M. Tentzeris, "Design and Optimization of 3D RF Modules, Microsystems and Packages Using Electromagnetic, Statistical and Genetic Tools", *2004 IEEE ECTC Conf. Dig.*, pp. 1412-1415, June 2004.

[10] D. Staiculescu, J. Laskar, E.M. Tentzeris, "Design Rule Development for Microwave Flip-Chip Applications", *IEEE Trans. Microwave Theory & Tech.*, Vol.48, No.9, pp.1476-1481, Sept. 2000.

[11] R.R. Tummala, J. Laskar: "Gigabit Wireless: System-on-a-Package Technology", *Proc. of the IEEE*, pp. 376 – 387, Feb. 2004.

[12] K. O'Connor, R. Libonati, J. Culver, D.H. Werner, P.L. Werner**: "**A planar spiral balun applied to a miniature stochastic dipole antenna" *2003 APS Int. Symp. Dig.*, pp. 938-941, June 2003.

[13] T. Rutkowski, W. Zieniutycz, K. Joachimowski: "Wideband coaxial balun for antenna application", *1998 International Conf. of Mirowaves and Radar*, pp. 389 – 392, May 1998.

[14] N.I. Dib, R.N. Simons, L.P.B. Katehi**: "**New uniplanar transitions for circuit and antenna applications", *IEEE Trans. Microwave Theory & Tech.*, Vol.43, No.12, pp.2868-2873, Dec. 1995.

[15] M.C. Tsai, "A New Compact Wideband Balun," *IEEE Microwave-Millimeter Wave Monolithic Circuits Symp. Dig.*, pp. 123-125, June 1993.

[16] K.W. Kobayashi, "A Novel HBT Active Transformer Balanced Schottky Diode Mixer," *2003 IEEE MTT-S Int. Microwave Symp. Dig.*, pp. 947-950, June 1996.

[17] H.-K. Chiou, H.-H. Lin, C.-Y. Chang, "Lumped-Element Compensated High/Low-Pass Balun design for MMIC Double Balanced Mixer," *1997 IEEE Microwave and Guided Wave Letters.* vol. 7, no. 8, pp. 248-250, Aug. 1997.

[18] B. Climer, "Analysis of Suspended Microstrip Taper Baluns," *IEEE Proceedings*, vol. 135, pt. H., no. 2, pp. 65-69, April 1998.

[19] A.M. Pavio and A. Kikel, "A Monolithic or Hybrid Broadband Compensated Balun," *1990 IEEE MTT-S Int. Microwave Symp. Dig.*, pp. 483-486, May 1990.

[20] JMP Version 5.0.1.2, SAS Institute Inc., Cary, NC, 2003.

[21] G. Derringer, R. Suich, "Simultaneous optimization of several response variables", *Journal of Quality Technology*, vol. 12, nr. 4, pp. 214-219, Oct. 1980.

[22] D.M. Pozar, *Microwave Engineering.* Wiley, 1998, pp. 352-353.

[23] K.S. Ang, I.D. Robertson*:* "Analysis and design of impedance-transforming planar Marchand baluns**",** *IEEE Trans. Microwave Theory & Tech*, Vol. 49 , No.2, pp. 402 – 406, Feb. 2001.